Opportunistic Routing and Scheduling for Wireless Networks

Weiwei Chen, Chin-Tau Lea, Shiming He, and Zhe XuanYuan

***Abstract*— In spatial time division multiple access wireless mesh networks, not all links can be activated simultaneously, as links scheduled for transmission must satisfy the specified SINR requirements. Previously, slot assignment has been done on a link basis, where a set of links is selected for transmission in a given slot. However, if selected links are in deep fade or have no traffic to transmit, the slot is wasted. Thus, a node-based scheme was proposed, where a set of nodes is selected for transmission. Which link to be used by a node depends on the links' instantaneous traffic load. Although this allows us to exploit multi-user diversity, it creates a planning discrepancy: slot assignment is designed based on long-term channel statistics, but scheduling on short-term channel fading conditions. Consequently, the performance gain of the node-based scheme is not consistent: it is marginal under certain scenarios. To avoid the design discrepancy, we develop a new slot-assignment and routing framework in this paper. The new approach incorporates short-term channel fading statistics to optimize the long term slot assignment, routing and scheduling simultaneously. Hence, multi-user diversity can be exploited more efficiently. Not only is the performance gain of the resulting system significant (can be as much as 64% higher throughput than the scheme introduced by Chen and Lea), it is also less topology dependent compared with the one by Chen and Lea.**

***Index Terms*— Opportunistic scheduling, multi-user diversity, multi-hop wireless networks, STDMA networks.**

I. Introduction

A WIRELESS mesh network [2] has two attractive attributes: fast deployment and low cost. Carrier Sense Multiple Access/Collision Avoidance (CSMA/CA) and Spatial Time Division Multiple Access (STDMA) are two protocols commonly used in such networks [2]. Nodes in a CSMA/CA network need not be synchronized, which makes it easier to deploy such a network. However, the hidden/exposed terminal problem [3] inherent in a multi-hop CSMA/CA protocol can significantly degrade the overall throughput. Nodes in an STDMA mesh network [4], [5] must be synchronized. Nevertheless, it can avoid the hidden/exposed problem through careful transmission planning. We focus on STDMA networks in this study.

Transmissions in an STDMA mesh network are organized into frames and each frame contains multiple slots. Links scheduled for transmission must satisfy a specified SINR requirement. Therefore, not all links can be activated in a slot, and a time slot assignment scheme is required of which the goal is usually to maximize the network throughput. In traditional slot assignment schemes [6]–[14], a set of links is selected for transmission in each slot. When a scheduled link is in deep fade or a selected link has no traffic to transmit, the slot given to that link will be wasted. To fix this problem, a ***node-based*** slot assignment scheme was proposed in [1] wherein a set of nodes, not links, is selected for transmission in each slot. Which link is to be selected by a node, however, will depend on the instantaneous channel fading and the traffic conditions of all the links attached to the transmitting node. Since a node has multiple links to schedule in one slot, a node-based scheme can exploit ***multi-user diversity*** in scheduling. Moreover, the node-based scheme is further discussed in [15] to minimize the energy consumption of a wireless network.

Whether the slot assignment scheme is link-based or node-based, the formulation of the problem is always based on long-term channel statistics and the short-term fading effects are usually ignored as it is too complicated to be included in the formulation. However, this creates a modeling discrepancy for a node-based scheme as its scheduling scheme is based on the short-term channel fading conditions, which are not included in routing and capacity planning. Due to this discrepancy, the performance gain of exploiting multi-user diversity by a node-based scheme is not consistent and sometimes only marginal. The gain is also highly topology dependent (see Sec. V).

We fix this problem in this paper by developing a new slot assignment, routing and scheduling framework. The new framework allows us to incorporate the short-term fading information into the long-term routing and slot assignment. It thus removes the modeling discrepancy mentioned above. Not only does the new scheme have significant performance gains over the conventional frameworks described in [6]–[14], the gains are also consistent and less topology dependent.

The contributions of the paper are the following. Firstly, we propose a new framework for jointly designing routing, slot assignment and scheduling algorithms for STDMA mesh

Manuscript received November 21, 2015; revised April 29, 2016; accepted October 14, 2016. Date of publication October 31, 2016; date of current version January 6, 2017. This work was supported in part by Hong Kong RGC under Grant 16206015 and in part by the National Science Foundation of China for Young Scholars under Grant 61501528. The associate editor coordinating the review of this paper and approving it for publication was W. Wang.

W. Chen is with the College of Computer Science and Electronic Engineering, Hunan University 410012, China (e-mail: avachen@hnu.edu.cn).

C.-T. Lea is with the Department of Electrical and Computer Engineering, The Hong Kong University of Science and Technology, Hong Kong (e-mail: eelea@ece.ust.hk).

S. He is with the Department of Computer Science, Changsha University of Science and Technology, Changsha 410114, China (e-mail: smhe_cs@ceust.edu.cn).

Z. XuanYuan is with the Beijing Normal University–Hong Kong Baptist University, United International College, Zhuhai, China (e-mail: zhexuanyuan@uic.edu.hk).

Color versions of one or more of the figures in this paper are available online at http://ieeexplore.ieee.org.

Digital Object Identifier 10.1109/TWC.2016.2623308

networks. Different from [1], the new approach incorporates short-term channel fading statistics to optimize the long-term slot assignment, routing and link scheduling ***simultaneously***. Not only is the performance gain of the resulting system significant, it is also less topology dependent compared with the scheme in [1]. Secondly, we apply the new approach to a practical OFDMA system to test the performance of the system. The tested system includes all important implementation details, such as scheduling, frame construction, and Channel State Information (CSI) overhead. The results show that the new framework can achieve a performance gain as high as 64.0% over existing approaches.

The rest of the paper is organized as follows. Sec. II discusses the general system model used in our analysis. Sec. III introduces the proposed slot assignment, routing and scheduling framework. Sec. IV discusses the details of the scheduling schemes for the proposed framework in an OFDMA system, and Sec. V presents the performance evaluation results. Sec. VI concludes the paper.

II. System Model

In this section, we present the system model on which the evaluation of the proposed scheme will be based. To show the practicality of the proposed framework, we will also discuss several implementation issues. In a wireless mesh backbone network, nodes' locations are stationary and traffic demand of the system is relatively stable [2]. For such a system, an STDMA scheme can achieve high throughput performance if slot assignment, routing and link scheduling are properly pre-planned. Multi-path routing is assumed in our study (e.g. Multi-protocol Label Switch based routing scheme). This, however, does not mean packets will be transmitted out of sequence as traffic splitting can be flow based.

A. Node Pattern

In this study, an STDMA system is assumed. Transmissions are divided into frames and the transmission pattern of a slot will be repeated frame after frame. Moreover, a set of nodes will be allowed to transmit in a given slot. Each node will then select one from a set of links to transmit in that slot. In each given slot, we define the set of nodes and the set of potential links attached to each node that can be selected for transmission as a node pattern. Let N be a node pattern. $N = \left\{(p^N, E_p^N)|\ p^N \text{ is a node selected to transmit and } E_p^N \text{ is the set of links of } p^N \text{ that can be selected for transmission in a given slot}\right\}$. Note that the set of transmitting node is fixed in a node pattern and which link to select by a transmitting node will not affect the interference profiles of other links in the same slot. Therefore, each node is able to make scheduling decision independently.

B. CSI Feedback Implementation

We assume OFDMA is used by the physical layer of the system [16] in which the spectrum contains l subcarriers, and the l subcarriers are further divided into m channels.

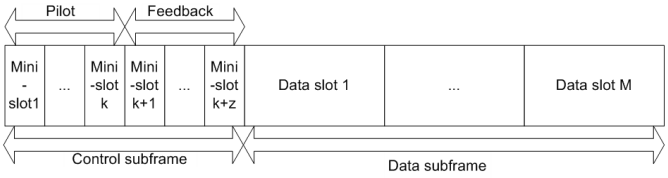

Fig. 1. Illustration of a frame structure.

Each channel consists of $\frac{l}{m}$ subcarriers. There are two subcarrier grouping schemes for a channel. The first scheme group adjacent subcarriers into one channel and the second scheme uses subcarriers distributed over the whole bandwidth to form a channel. We use the first scheme for data channels as this allows us to exploit multi-user diversity, and the second scheme for sending CSI as it can average the impact of the fading of each sub-carrier.

Adaptive Modulation and Coding (AMC) scheme is adopted in the system where different channels, depending on their interference and fading conditions, can have different transmission rates. With AMC, a data packet is usually assumed to be fragmented into multiple segments and a segment can fit into a slot of the lowest transmission rate. To facilitate AMC, CSI feedback is required. Since the locations of nodes (mesh routers) are stable, the coherence time of the wireless channels between different mesh routers is usually in the range from tens to hundreds of milliseconds [17], [18]. Hence it is reasonable to feedback CSI on a frame basis. Notice that, to make sure the CSI is up to date, the frame length is set to be no longer than the minimal coherence time of all the channels in the system. This can be easily achieved by setting an appropriate frame length.

To facilitate the above discussion, a frame is divided into a control and a data sub-frame (see Fig. 1). The data sub-frame consists of multiple data slots, which are used for data transmission. The control sub-frame consists of multiple mini-slots which are divided into two parts, one for sending pilot signals and one for sending CSI feedback. Each node pattern uses one mini-slot for sending pilot signals—all active nodes in a node pattern will transmit pilot signals simultaneously to their attached links. After receiving pilot signals, receivers of the links will estimate the highest modulation schemes they can use and send the information back through the mini-slots of the CSI feedback portion. This CSI feedback of each link may take several mini-slots to transmit, and the transmissions are also done with a pre-determined pattern. The details are shown in Appendix-A. In Section V (the simulation part), we will discuss the CSI feedback overhead.

C. Effective SINR and the State of a Transmitting Node

One of the key ideas in this study is that a transmitting node should conduct different link scheduling when the set of links attached with that node experience different channel fading condition. To incorporate this short-term design into the long-term planning, we will introduce two concepts in this subsection to facilitate our discussion: effective SINR and a state of a transmitting node.

1) Effective SINR: Power control, similar to many deployed wireless systems, is not used in this study. In an OFDMA system, as mentioned in the previous subsection, the whole bandwidth is divided into several channels and each channel contains multiple sub-carriers. The bandwidth of each subcarrier is small enough to justify the assumption of flat fading for each sub-carrier. The statistical fading model for each sub-carrier consists of three major components: path loss, shadowing and fast fading. Let tx and rx be the intended transmitter and receiver. The path loss between tx and rx is modeled as $l_{rx,tx}^{-\alpha}$, where $l_{rx,tx}$ is the distance between tx and rx and α is a constant which usually varies from 2 to 4. The shadowing effect is modeled as $10^{\frac{f_{rx,tx}}{10}}$, where $f_{rx,tx}$ is a normal distributed random variable. Rich scattering environment and a block-wise Rayleigh distribution [19] are assumed for each sub-carrier. With this, the instant received power of sub-carrier k of rx from tx is $\zeta_{rx,tx,k} = l_{rx,tx}^{-\alpha} \cdot 10^{\frac{f_{rx,tx}}{10}} \cdot p_{tx} \cdot \pi_{rx,tx,k}$. Here $\pi_{rx,tx,k}$ is a Rayleigh distributed r.v. (with mean = 1). Moreover, since the location of each mesh router is stable, we assume that the shadowing effect between two nodes remains the same and do not change over time. Hence, once $f_{rx,tx}$ is given, $\zeta_{rx,tx,k}$ can be modeled as a Rayleigh distributed r.v. (with mean $= l_{rx,tx}^{-\alpha} \cdot 10^{f_{rx,tx}/10} \cdot p_{tx}$). Let $\gamma^{N,e,k}$ be the SINR of sub-carrier k of link e in node pattern N. That is

$$\gamma^{N,e,k} = \frac{\zeta_{rx,tx,k}}{\sum_{\{i|i\in\{N\setminus tx\}\}} \zeta_{rx,i,k} + \omega}, \tag{1}$$

where $e \in E_{tx}^N$ and ω is the power of the thermal noise.

In most practical systems, all sub-carriers of a channel will be assigned with the same modulation scheme in order to reduce the channel state information feedback. To determine the modulation scheme suitable for a channel, the concept of effective SINR has been proposed and widely used [20]. Effective SINR tries to capture the overall SINR behaviors of all the sub-carriers of a channel. It works in the following way. Let Sub represent the set of sub-carriers of a channel. If this channel uses modulation b, its effective SINR in link e, denoted by $\tilde{\gamma}_b^{N,e}$, can be expressed as:

$$\tilde{\gamma}_b^{N,e} = -\beta_b ln\left(\frac{\sum_{i\in Sub} exp(-\frac{\gamma^{N,e,i}}{\beta_b})}{|Sub|}\right). \tag{2}$$

Here $|Sub|$ is the cardinality of the set Sub, and β_b, a pre-determined parameter, is uniquely determined by the modulation scheme b.

Given a required block error rate (set to 10% in this study), we can use the effective SINR threshold to map the current effective SINR to the transmission rate for a channel. Let th_i be the effective SINR thresholds for the ith modulation scheme (note that $th_i < th_j$ if $i < j$). A channel will use modulation scheme i if $\tilde{\gamma}_i^{N,e} \geq th_i$. Thus the modulation scheme used on link e for a channel will be the maximum j such that its $\tilde{\gamma}_j^{N,e} \geq th_j$. Let ξ be the number of modulation schemes and $\{th_1, th_2, \cdots, th_\xi\}$ be the effective SINR thresholds for the corresponding data rates of the modulation schemes for a channel. Let $q_l^{N,e}$ represent the probability that a channel will use modulation scheme l ($1 \leq l \leq \xi$). Obviously, we have

$$q_l^{N,e} = Pr\left(th_l \leq \tilde{\gamma}_l^{N,e} < th_{l+1}\right) \tag{3}$$

where $q_l^{N,e}$ is required for solving our problem and $th_{\xi+1} = \infty$. To compute $q_l^{N,e}$, we need the distribution of $\tilde{\gamma}_l^{N,e}$. To derive this probability distribution, we approximate the interferences and the thermal noise of a link as a Gaussian random variable. With this, (1) becomes

$$\gamma^{N,e,k} \approx \frac{\zeta_{rx,tx,k}}{\sum_{\{i|i\in\{N\setminus tx\}\}} l_{rx,i}^{-\alpha} \cdot 10^{f_{rx,i}/10} \cdot p_i + \omega}. \tag{4}$$

Notice that in (4), given the shadowing effect $f_{rx,i}$, the Rayleigh distributed interferences ($l_{rx,i}^{-\alpha} \cdot 10^{f_{rx,i}/10} \cdot p_i \cdot \pi_{rx,i,k}$) in the denominator are approximated as fixed numbers ($l_{rx,i}^{-\alpha} \cdot 10^{f_{rx,i}/10} \cdot p_i$). There are two reasons why we approximate Rayleigh distributed interferences with fixed numbers. Firstly, we need a close-form formula of the effective SINR distribution to efficiently plan routing and scheduling for the network. But as pointed out in [20], deriving such a formula with Rayleigh distributed interferences would be extremely difficult. Secondly, according to the results shown in both [20] and our results presented in Sec. V-B.2, the impact of this approximation on the final results is marginal, which justifies the approximation approach.

Denote $w = exp(-\tilde{\gamma}_l^{N,e}/\beta_l)$. Let $E(w)$ and $Var(w)$ be the expectation and the variance of w, and $a_l^{N,e} = \frac{E(w)(E(w)-E(w^2)-Var(w))}{Var(w)}$, $b_l^{N,e} = \frac{1-E(w)}{E(w)} a_l^{N,e}$. The detailed expression of $E(w)$ and $Var(w)$ are given in Appendix B. According to [21], the sum of i.i.d. RVs. with finite support can be approximated by a Beta distributed random variable. We will follow the same idea and approximate the effective SINR as a Beta distributed random variable. Hence $q_l^{N,e}$ is:

$$q_l^{N,e} \approx B_i(e^{-\frac{th_l}{\beta_l}}, a_l^{N,e}, b_l^{N,e}) - B_i(e^{-\frac{th_{l+1}}{\beta_{l+1}}}, a_{l+1}^{N,e}, b_{l+1}^{N,e}) \tag{5}$$

Here $B_i(\cdot,\cdot,\cdot)$ represents the incomplete Beta function. Later our simulation results will show that $q_l^{N,e}$ derived from this model is very close to the simulation results. As will be discussed in Sec. V, the overall throughput gap between the approach using the approximated and the real distribution of $\tilde{\gamma}_b^{N,e}$ is marginal, which indicates that the approximated approach is suitable for our analysis.

2) The State of a Transmitting Node: Scheduling in an OFDMA system is done on a per-channel basis. Since the distributions of the fast fading component of all the subcarriers are identical, we assume all the data channels have identical EESM distributions. Node p in N can allocate a channel to any link $e \in E_p^N$, and the allocation often depends on the modulation scheme that can be used for a link. Thus given the (N, p) tuple, we define the state of a channel as a tuple s_p^N, where $s_p^N = \{d_e | d_e$ is the highest modulation scheme can be used for this channel on link $e, e \in E_p^N\}$. E.g., if $|E_p^N| = 2$ and there are four modulations for each link, then there are 16 different states for any channel in node p. This shows that the number of states of a channel grows exponentially with the number of modulations used in the system. To reduce the

TABLE I
NOTATIONS

V	The set of nodes in the system.
E	The set of links in the system.
NP	The set of node patterns in the system.
F	The set of flows in the system $F = \{f\}$.
h_f	The traffic demand for flow f.
x_{fe}	The portion of traffic routed through link e for flow f.
r	Throughput scaling parameter.
tx_e/rx_e	The transmitter and receiver of link e.
m	The number of data channels of a link.
E_p^N	The set of links that can be activated by node p, where p is a transmitting node in node pattern N.
θ^N	The portion of time assigned to node pattern N in a frame.
s_p^N	The state of a channel of transmitting node p, given (N, p) and p is a node in node pattern N.
$g(s_p^N)$	The probability that any channel of node p in node pattern N is in state s_p^N.
$c_e(s_p^N)$	The data rate of a channel when it is assigned to link e, given the channel state s_p^N and $tx_e = p$.
$\mu_e(s_p^N)$	The portion of time assigned to a channel of link e when the state of this channel is s_p^N.

number of states for a transmitting node in each channel, we can group different modulation schemes into one. All the discussion above, nevertheless, remains unchanged. Let $g(s_p^N)$ be the probability for a channel to be in state s_p^N. Since the fading characteristics of different links are independent, we have

$$g(s_p^N) = \prod_{\{e \in E_p^N\}} q_{d_e}^{N,e}. \tag{6}$$

III. New Design Framework for Routing and Opportunistic Scheduling

In this section, we will discuss how to design routing and scheduling with the proposed framework. The main difference between the proposed framework and the prior frameworks is that the former can incorporate short-term fading statistics in routing/slot assignment and scheduling. This design difference, as demonstrated in Sec. V-B, can make a huge performance difference. The notations are shown in Table I.

A. Formulation of the Proposed Opportunistic Scheduling and Routing Scheme

A flow is defined as a (source, destination) pair. Denote f as a flow, src_f and dst_f as the source and destination of flow f. Let h_f be the traffic demand of flow f, which is a given parameter and implies the traffic unevenness among all the flows in the network. For example, if $h_1 = 1$, and $h_2 = 2$, it means the traffic demand of flow 2 is twice that of flow 1. If $h_f = 1, \forall f \in F$, the derived framework will provide the same amount of throughput for all flows. The real throughput of a flow in the network is represented by rh_f, where r, a scaling parameter, is a variable we intends to maximize. To maximize r is to maximize the minimal throughput of all the flows in the network. Let $\{x_{fe}\}$ be the portion of traffic of flow f routed through link e. This is the routing parameter of the network. With this, network conservation constraints is

$$\sum_{\{e|tx_e=v\}} x_{f,e} - \sum_{\{e|rx_e=v\}} x_{f,e} = \begin{cases} 0, v \neq src_f, dst_f, \\ r, v = src_f, \\ -r, v = dst_f. \end{cases} \tag{7}$$

Conventional link-based scheduling algorithms [6]–[14] use long-term channel statistics to design the short-term scheduling algorithm. The discrepancy, as shown later, leads to a huge performance gap. To solve this problem, we introduce the scheduling parameter $\mu_e(s_p^N)$, which is the portion of time that a channel is assigned to link e ($e \in E_p^N$) when the channel is in state s_p^N. With $g(s_p^N)$ (the probability for a channel to be in state s_p^N) and $\mu_e(s_p^N)$, we can use different scheduling strategies for different link states. This allows us to incorporate channel fading into network routing and scheduling design. To make sure that the total amount of bandwidth link e receives is less or equal to the total amount of traffic routed through e, the following should hold:

$$\sum_{f \in F} h_f x_{fe} \leq m \sum_{\{N, s_p^N | e \in E_p^N\}} g(s_p^N) \mu_e(s_p^N) c_e(s_p^N). \tag{8}$$

Here m represents the number of data channels in the OFDMA system, and $c_e(s_p^N)$ the data rate of a channel assigned to link e if node p in node pattern N is in state s_p^N. In other words, $c_e(s_p^N)$ is the data rate of a channel when it uses modulation scheme d_e with $d_e \in s_p^N$.

Since the total amount of time assigned to all the links in E_p^N under different states is less than or equal to the amount of time assigned to node pattern N. We have

$$\sum_{e \in E_p^N} \mu_e(s_p^N) \leq \theta^N, \qquad \forall s_p^N. \tag{9}$$

Likewise, the network feasibility constraint is

$$\sum_{N \in NP} \theta^N = 1. \tag{10}$$

Put everything together, we can use the following formulation to maximize the throughput scaling parameter r.

$$\max \quad r \tag{11a}$$

$$\text{s.t.} \quad (7), (8), (9), (10). \tag{11b}$$

To solve (11), we need to compute $g(s_p^N)$ and the distribution of $\tilde{\gamma}_b^{N,e}$. This distribution is difficult to derive analytically. We can use simulation to get $\tilde{\gamma}_b^{N,e}$, but there are many node patterns to make the simulation approach practical. Instead, we use a two-phase approach to tackle this problem. In phase 1, we use the approximated distribution of $\tilde{\gamma}_b^{N,e}$ as discussed in Sec. II-C to derive $g(s_p^N)$ and solve (11). This result includes a set of node patterns to be used in the system. The number of selected patterns is in the range of tens. In phase 2, we use simulation to derive a more accurate distribution of $\tilde{\gamma}_b^{N,e}$ for the set of node patterns derived in phase 1 and resolve $g(s_p^N)$ and (11). Since the selected number of node patterns for slot assignment is small, the computational complexity of the simulation approach is acceptable. As will be shown in Sec. V, the overall throughput gap between the simulated SINR distribution and the approximated one is only marginal. This indicates (4) offers a good approximation for $\tilde{\gamma}_b^{N,e}$.

B. Column Generation Algorithm

As the number of node patterns increases, listing all node patterns as done in (11) is not scalable because the number of node patterns and states grow exponentially with the network size. Column generation uses only a subset of variables to solve an LP. For our problem, the algorithm decomposes the problem into a master and a sub-problem. In the master problem, it solves the LP with a selected subset of node patterns. Since the number of node patterns in the master problem is much smaller than that of the original problem, we can resolve the master problem easily. In the sub-problem, we use duality theory to verify the optimality of the master problem and select a new node pattern and add it to the master problem later to improve the result.

Phase-I: Master problem

The master problem is the same as (11), except that the variable set will be redefined as $\{\theta^N | N \in NP'\}$ and $\{\mu_e(s_p^N) | N \in NP', e \in E_p^N, p \in N\}$. Here NP' is a subset of NP which is feasible for (11). By resolving the master problem, we get the result which is optimal for NP', not NP. To justify whether a new pattern can improve the mater problem and hence be added into NP', we first take the dual of (11) to obtain dual variables $\{\sigma_f\}$ for the constraint (7) in (11). The dual of (11) can be expressed as

$$\max \quad \delta \tag{12a}$$

$$\text{s.t.} \quad 1 - \sum_{\{f \in F\}} \sigma_{f,src_f} + \sum_{\{f \in F\}} \sigma_{f,dst_f} \geq 0, \tag{12b}$$

$$\delta - \sum_{s,p \in N} \phi_{ps}^N \geq 0, \tag{12c}$$

$$\phi_{ps}^N - mg(s_p^N)\tau_e c_e(s_p^N) \geq 0, \tag{12d}$$

$$\tau_e h_f + \sigma_{f,tx_e} - \sigma_{f,rx_e} \geq 0. \tag{12e}$$

After resolving (12), $\{\sigma_f^v\}$ will be used in the sub-problem to test the optimality of the master problem.

Phase-II: Sub-problem

In this phase, the algorithm verifies the optimality of the master problem and adds new node patterns into NP' if the master problem is not global optimal. We first denote $\tau_e = \max_f(\sigma_{f,tx_e} - \sigma_{f,rx_e})/h_f$. τ_e can be found once (12) is resolved. For a new $N(N \notin NP')$, let $\phi_{ps}^N = m \cdot \max_{e \in E_p^N} g(s_p^N)\tau_e c_e(s_p^N)$. We further define the reduced price of N as $rp^N = \sum_{\left\{p \in t^N, s \in S_p^N\right\}} \phi_{ps}^N$. According to the duality theory, the optimal result of the primal problem (11) and the dual problem (12) will converge to the same value. This implies that if constraints (12c-12d) can be satisfied by all the node patterns or $rp^N \leq \delta$ for all $N \in NP$, adding new node patterns into (12) will not reduce its optimal value and (12) has already converged to its minimum value. Consequently, the master problem has already reached its maximum value with the current node pattern set NP'. On the other hand, as long as there exists a node pattern N, such that $rp^N > \delta$, adding node pattern N into NP' has the potential to improve the master problem.

In the sub-problem, among all the node patterns not in NP', we will choose the one with the largest rp^N and add it into NP' if $rp^N > \delta$. The column generation algorithm will iterate between the master and the sub-problem until $rp^N \leq \delta$ for all possible node patterns. However, the improvement is usually steep initially, but wanes as the number of iterations increases. The stopping condition we set to the algorithm is $rp^N < (1 + \triangle)\delta$ for all node patterns. ($\triangle$ is a sufficiently small positive value, and we set it to be 0.01.)

C. Reducing the Computational Complexity of the Problem

The complexity of (11) is also related to the number of states of a channel (see (8) and (9)), which is strongly affected by the number of links attached to a node in a given slot. Although the number of states s_p^N grows exponentially with $|E_p^N|$, some states have negligible $g(s_p^N)$. We can ignore those states with small probabilities. The detailed procedure to exclude the negligible $g(s_p^N)$ is discussed in Appendix C. Let e_{max} be the maximum number of links allowed for $|E_p^N|$. This parameter represents the trade-off between computational complexity and the system performance. Even though the throughput gain due to the increase of e_{max} is diminishing fast. We can keep e_{max} small and still achieve a good performance for the system. We will discuss the impact of different $|E_p^N|$ on the system throughput in Sec. V.

In addition, in the sub-problem of the column generation method, we need to select a node pattern to improve the master problem. However, the complexity of the pattern selection procedure grows exponentially with the number of nodes in the network. Hence we will use a heuristic algorithm for node pattern selection to reduce the complexity. The algorithm is also listed in Appendix C and discussed in the simulation parts (Sec. V). Note that when the network is large, even column generation cannot lead to the optimal solution because it is impossible to exhaustively search all node patterns and find the one with the most negative reduced price. This problem is not unique for our proposed framework. The traditional link-based scheme [7] and the node-based scheme proposed in [1] also have this problem.

D. Frame Construction

When the proposed opportunistic routing and scheduling scheme is calculated, the optimal slot assignment is determined. However, we need to construct a frame in which the number of slots assigned to a pattern reflects the portion of time derived from (11) (θ^N). To quantize the portion of time assigned to a node pattern to an integer value, we use the method proposed in [1] and set $n_f = \sum_{N \in NP} round(z \cdot \theta^N)$. Here z is the intended frame length, n_f is the final frame length and the function $round(x)$ rounds x to its neatest integer. Moreover, the quantized portion of time assigned to each slot in a frame becomes $\tilde{\theta}^N = \frac{round(z \cdot \theta^N)}{n_f}$. Since $\tilde{\theta}^N$ has changed, we then use the new $\tilde{\theta}^N$ to re-optimize the routing and scheduling scheme as follows:

$$\max \quad r_z \tag{13a}$$

$$\text{s.t.} \quad \sum_{e \in s_p^N} \mu_e(s_p^N) \leq \tilde{\theta}^N \tag{13b}$$

$$(7), (8) \tag{13c}$$

The optimization will be done for the range $z_{min} \leq z \leq z_{max}$. The z resulting in the highest value of r_z will be used. That is, $r_{max} = \max_{z_{min} \leq z \leq z_{max}} r_z$.

IV. Scheduling Implementation of the Proposed Framework

The slot assignment and routing scheme discussed in the previous section is computed off-line and can remain unchanged for a long period of time as the traffic demand in a wireless mesh backbone network is relatively stable [2]. The link scheduling, on the other hand, needs to be done online. In this section, we will explore two scheduling schemes for implementing the proposed framework. The two have a similar performance, but have very different complexities.

When doing real scheduling, a node will firstly collect the supportable modulation scheme from its attached links. The overhead of the data rate feedback is small (see appendix D). After gathering the information of the supportable modulation scheme, a transmitting node will schedule its attached links without any coordination among other transmitting nodes. In other words, scheduling can be realized in a totally distributed fashion. Moreover, scheduling is done on a per-channel basis.

A. Scheduling Scheme-I:

The first scheduling implementation conforms to the transmission probabilities ($\mu_e(s_p^N)$) derived from (11). Each node needs to store all the transmission probabilities in node patterns used in a frame. When node p is activated in N, it first uses the CSI feedback to determine the state s_p^N it is in for a channel. It then generates a random number between 0 and 1 for that channel and uses $\mu_e(s_p^N)$ to determine the range of the random number for selecting or not selecting a link.

B. Scheduling Scheme-II:

Sheme-II intends to achieve a similar performance to Scheme I without using the transmission probabilities $\mu_e(s_p^N)$ by each node. It is based on the idea of shadow queues [22].

To implement a shadow queue, we only need to include a real variable to store the length of a shadow queue. Let $q_e(x)$ and $q'_e(x)$ be the length of the real queue and of the shadow queue of link e. Since we only discuss the management of the shadow queue of link e, we will drop e and use $q(x)$ and $q'(x)$ in the discussion below. Recall that scheduling is done on a channel-basis. After a channel, say k, has been scheduled in slot x, we update $q(x)$ and $q'(x)$ as follows.

$$q(x) = q(x-1) + a(x) - d(x), \tag{14a}$$

$$q'(x) = q'(x-1) + a'(x) - d'(x). \tag{14b}$$

Here $a(x)$ and $a'(x)$ are the number of arrivals, $d(x)$ and $d'(x)$ are the number of departures of the data and shadow queue in slot x. $a'(x)$ is given by $a'(x) = \frac{1+\epsilon}{x} \sum_{t=0}^{x} a(t)$, where $\epsilon > 0$ is a sufficiently small positive number. $a'(x)$ represents the smoothed arrival rate and $q'(x)$ is the queue length after smoothing. Denote the instant rate of channel k in slot x as $\tilde{c}_k(x)$. Obviously, $d(x) = \min\{\tilde{c}_k(x), q(x)\}$ must hold. Thus we set $d'(x)$ as $d'(x) = \min\{\tilde{c}_k(x), q'(x)\}$.

Notice that, the incoming rate of a shadow queue ($a'(x)$) is a much smoother estimate of the real incoming rate as $a'(x)$ is achieved by passing $a(x)$ through a low pass filter. The reason to use the shadow queue is to avoid potential system instability due to the drastic variations of the incoming rate.

In Scheme II, the incoming packets for each link are separated into different data queues based on the number of hops a flow has already passed through [22]. These queues, however, share the same storage space. Each queue has a head and tail pointer plus the shadow-queue length variable. A queue is selected for transmission if it has the maximum (shadow queue length times the instantaneous rate). By doing so, the scheduler is able to strike the balance between system fairness (i.e. the shadow queue length parameter) and throughput (i.e. instant transmission rate of a channel). As has been shown in [22], the shadow queue-based scheduling scheme can achieve the highest throughput performance with a given routing scheme. Consequently, scheme-II, with a much lower implementation complexity, can achieve the same throughput performance as that of scheme-I without requiring a transmitting node to remember all the transmission probabilities $\mu_e(s_p^N)$.

V. Performance Evaluations

In this section, we compare the performances for several approaches, including the proposed one. We intend to show that by incorporating the instant channel fading statistics into the slot assignment and routing planning, we can achieve significant performance gains over existing approaches. We compare the delay/throughput performance as follows.

1) Framework-A (i.e. the traditional link-based scheme): Routing and slot assignment are designed based on the long-term channel statistics (formulation is given in (15) in Appendix A). Moreover, static scheduling derived from the routing and slot assignment scheme is used.
2) Framework-B (i.e. the one proposed in [1]): Routing and slot assignment are designed based on the long-term channel statistics (formulation is given in (21) in [1]). The scheme does not consider short-term channel fading statistics. Furthermore, dynamic scheduling based on the short-term fading behaviors of the channels (similar to Scheme-II in this study) is used.
3) Framework-C (the one proposed in this study): Routing and slot assignment are based on (11). Likewise, scheduling scheme-I and scheme-II of Sec. IV are used.

A. System Description

The topologies for evaluation are given in Fig. 2. The SINR threshold and β for different modulation schemes (refer to Sec. II-C) is provided in Table II [20]. We will use the SINR mapping table and (3) to determine the probability of a state in a given slot. Also a node can transmit an integer number of packets in a slot. The system parameters are set according to [23]. To be specific, the transmission power and the thermal noise is 20dBm and -90dBm. The total bandwidth is set to 10MHz, which is divided into 1024 sub-carriers. Moreover,

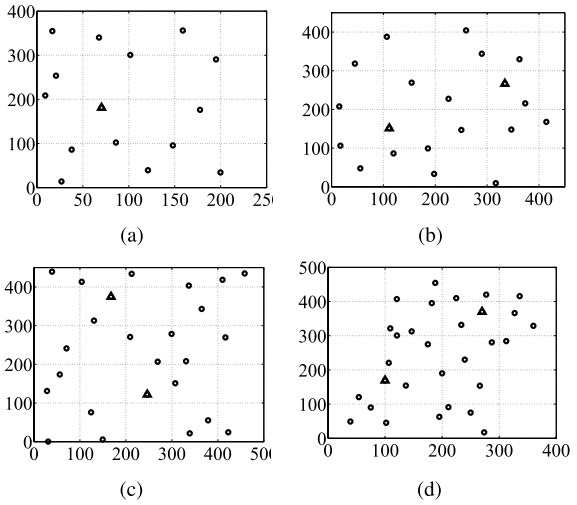

Fig. 2. Topology of the: (a) 15-node network; (b) 20-node network; (c) 25-node network;(d) 30-node network.

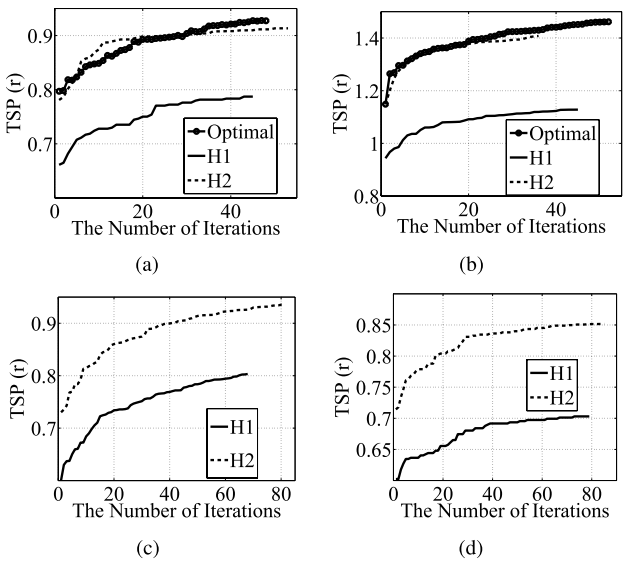

Fig. 3. Throughput of Framework A and of Framework C with the proposed column generation method derived from the analysis: (a) 15-node network; (b) 20-node network; (c) 25-node network; (d) 30-node network. Here TSP stands for Throughput Scaling Parameter

TABLE II
β VALUE AND SINR THRESHOLDS (WITH BLER=0.1)

Modulation Scheme	Effective rate	β	SINR threshold (dB)
64QAM 5/6	5bits/s/Hz	41.5	18.89
64QAM 3/4	4.5bits/s/Hz	41.0	17.51
64QAM 2/3	4bits/s/Hz	40.5	16.79
16QAM 3/4	3bits/s/Hz	9.6	11.54
16QAM 1/2	2bits/s/Hz	9.58	8.40
QPSK 3/4	1.5bits/s/Hz	1.75	4.77
QPSK 1/2	1bit/s/Hz	1.66	1.65

840 sub-carriers are used for data transmission. The number of sub-carriers in a channel is set to 24, which is in accordance with the number of sub-carriers of a channel in an LTE system. The channelization method is set according to Sec. II-C. The channel model follows the instruction of [24]. Here we choose the environment as the Pedestrian B model. We also choose 0.5ms as the regular data slot size. Likewise since only a small amount of information is carried by a mini-slot, similar to IEEE 802.11 [25], the mini-slot size is set to a number that is smaller than a data slot. In our simulation we set it to $50\mu s$.

We then compare the delay/throughput performances of the three frameworks listed above with six different network sizes: 15-node, 20-node, 25-node and 30-node. System throughput is represented by the scaling parameter r in (11). Recall that the real throughput is rh_f, where h_f—the given parameter, describes the relative traffic intensity of each node. We set $h_f = 1$Mbps in the discussion below. We use the gateway traffic model [26] for evaluation where traffic only exists between gateway nodes (denoted as triangles in Fig. 2) and non-gateway nodes (denoted as circles in Fig. 2).

Performance evaluations are done in two different styles. First, we compare the performances derived from the analytical model developed in Sec. III. By ignoring the implementation details (use the simulated distribution of the effective SINR of a channel for (11) and do not consider CSI feedback as well as quantization loss due to frame construction), we can get some intuitive understanding about the performance differences among the various frameworks. We then compare the performances of the three frameworks based on a practical OFDMA system. In this endeavor, we use both analysis and simulations for evaluating the performances.

B. System Performances

1) The Performance of the Heuristic Algorithm for Selecting Node Patterns in the Column Generation Method: We first study the effectiveness of the heuristic approach for selecting a node pattern in column generation. Fig. 3 plots the number of iterations verses the throughput scaling parameter of the proposed opportunistic routing and scheduling framework (Framework-C) for the 4 networks shown in Fig. 2. In the figure, TSP is an abbreviation for Throughput Scaling Parameter. The throughputs, derived from Framework-C, are represented as a function of the number of steps used in column generation. In the figure, TSP represents the throughput scaling parameter. In Fig. 3(a)-3(d), we intend to show the performance gap between the optimal and the proposed heuristic algorithm of the proposed framework. The optimal solution is obtained via testing all possible node patterns in every iteration until the algorithm converges. The heuristic approach uses the techniques discussed in both Sec. III-C and Appendix C to get an efficient sub-optimal solution. Here the H1 curve shown in the figure represents the case when $\{e_{max} = 2, y = 2\}$. Here y is the number of modulation scheme groups and e_{max} is the maximum number of links attached with a transmitting node. It implies the scheme with the lowest computational complexity and the lowest throughput performance. Moreover, to reduce the computational complexity, we limit the maximum number of attached links of a node to 6. Hence the case with $\{e_{max} = 6, y = 8\}$ (denote as H2 in Fig. 3(a)-3(d)) show the highest computational complexity and the highest throughput performance in our evaluations. The impact of different y and

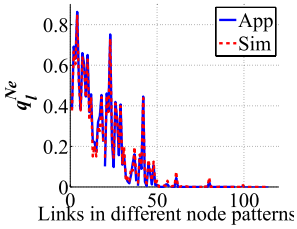

Fig. 4. $q_l^{N,e}$ of all the links in different node patterns of the 15-node network.

e_{max} on the overall system performances will be discussed in Sec. V-B.3. In Fig. 3(c)-3(d), we only show the results derived from the proposed heuristic algorithm because the number of node patterns in a 25-node or 30-node network is extremely large and the computational complexity is also tremendous. The results indicate that the throughput of the heuristic approach ranges from 84.4% to 98.5% of the optimal approach, and that both approaches will converge within several tens of column-generation steps for the tested topologies. It implies that the problem can be resolved efficiently by column generation algorithm.

2) The Impact of the Approximated EESM Distribution Model on System Throughput: Recall $q_l^{N,e}$ is the probability link e will use modulation scheme l to transmit data when it is activated in node pattern N. Fig. 4 shows $q_l^{N,e}$ of all the links in different node patterns for the 15-node network. In this figure, y and e_{max} is set to 2 and 6 respectively. In Fig. 4, the solid line indicates $q_l^{N,e}$ obtained from simulations (refer to (3) in Sec. II-C), and the dash line shows the results derived from the approximated EESM distribution (refer to (6) in Sec. II-C). We can observe that the differences between the two are marginal. Our study also indicates this conclusion will not be changed for different topologies or different y and e_{max}.

In terms of the throughput scaling parameter, the differences of the two models vary from -2.3% to 2.5% for different topologies and different y and e_{max}. This also indicates that the approximated EESM model offers a good approximation to the exact model.

3) The Impact of the Different Parameters on System Throughput: We compare the throughput derived from (11). Note that the throughput is derived based on the re-adjusted distribution of $q_l^{N,e}$ (the distribution is derived from simulation) according to the method discussed in Sec. III-A. Since the main difference between Framework-A and Framework-B is that the latter can exploit multi-user diversity in scheduling packets, if we were to ignore the implementation and focus only on the analytical results, there would be little performance difference between the two. Thus in this part, we only compare the performances of Framework-A and Framework-C.

There are several parameters that can affect the computational complexity and performance of a network. One is the maximum number of neighbors, denoted by e_{max}, allowed for a node in a given node pattern. The idea of limiting e_{max} is the following. If a node, for example, has four neighbors, we can set e_{max} to 2 and use two links in one slot and the other two links in another slot. This can significantly

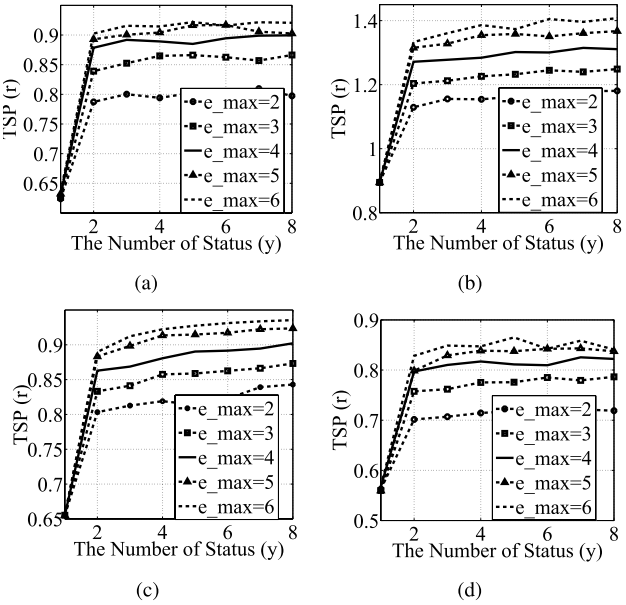

Fig. 5. Throughput of Framework A and of Framework C under different y and e_{max}: (a) 15-node network; (b) 20-node network; (c) 25-node network; (d) 30-node network.

reduce the computational and implementational complexity of the scheduling algorithm. But we like to know its negative impact on throughput. The other parameter is the number of modulation scheme groups, denoted by y. Although the system may have, say, four modulation schemes, we can group them into two and use (11) to compute the probabilities of each grouped modulation scheme, and the grouped modulation schemes are then used to solve the routing and slot assignment problem. This parameter also presents a complexity-performance tradeoff for the implemented system.

Fig.5 shows the throughput of Framework-C under different e_{max} and different y. From Fig. 3 and Fig. 5, we can observe that use a small e_{max} and y will only lead to little performance degradation. For instance, with $e_{max} = 4$ and $y = 2$ the throughput of the proposed heuristic algorithm is only 6.8%(15-node) and 13.0% (20-node) less than that of the same network with no constraint on e_{max} and no grouping on y.

Moreover, from Fig. 5, we can also observe that the proposed Framework-C has a significant throughput gain over the conventional Framework-A (all the points with $y = 1$). For instance, with $\{e_{max} = 6, y = 8\}$ for the 4 tested networks, compared with Framework-A, the proposed Framework-C has a throughput gain of 44.5% (15-node), 57.4% (20-node), 42.8% (25-node) and 55.2% (30-node), and a throughput gain of 25.4% (15-node), 26.2% (20-node), 22.6% (25-node) and 25.0% (30-node) when$\{e_{max} = 2, y = 2\}$.

4) Performances With Implementation Details: We use the OFDMA system described in Sec. II as the base for our comparison. The steps we take for implementing the system are the following:

1) Use (11) to derive the set of node patterns that will be used in a frame.
2) For each node pattern derived in Step 1, use Mont Carlo simulation to derive the probability of a state of a channel for any transmitting node (see Sec. II-C).

3) Use the set of node patterns (step 1) and the simulated state distributions (step 2) to re-optimize the routing and scheduling scheme according to (11).
4) Based on the results of Step 3, construct a data sub-frame according to (13) and a control sub-frame according to Appendic A. The two sub-frames are separated in the time domain.
5) Implement the static scheduling scheme for Framework-A, the Scheme-II scheduling algorithms for Framework-B (see Sec. IV) and the two scheduling algorithms in Sec. IV for Framework-C.

For brevity, in this subsection, we only present the results with $\{e_{max} = 6, y = 8\}$ for the 14 tested networks. For all the topologies we tested, the quantization loss due to frame construction and the overhead of the control sub-frame in the three frameworks are close to each other. The quantization loss (discussed with more details in [1]) in frame construction ranges from 0.2% to 7.2% for the tested topologies. The overhead of the control sub-frame ranges from 0.5% to 8.9% for all the tested topologies. More detailed information is provided in Appendix D.

Simulation is used to study the delay/throughput performances of the three different frameworks, where packets arrivals are assumed to follow a Poisson stream. The delay is represented by the average queue length of the bottleneck link (i.e. the most congested link) of a network. From Little's Theory, the average queuing delay of the link can be derived easily from this parameter. Each point reported in the figures below represents the average result of 10 simulation runs. Fig. 6 shows the delay/throughput performances of the three frameworks. In the figure, curve A denotes for the curve for Framework-A, B for Framework-B and C for Framework-C. Also the maximum achievable throughputs for all the topologies are listed in Table III in Appendix D. Note that the throughput of a framework in Fig. 6 is lower than that of the same framework in Fig. 5. This is because the latter does not consider the overhead associated with each step of the implementation, as described above. Let's compare Framework-A and Framework-B first. Recall that both do not consider instant channel fading in routing and slot assignment, but Framework-B can consider fading in scheduling. This allows the system to exploit multi-user diversity in scheduling packets. We can see that a throughput gain over Framework-A are 26.1%, and 9.9% for the 15-node and the 25-node network. However, there is little gain for the 20-node and 30-node network. This is the point mentioned in the introduction. If we do not consider fading statistics in routing and slot assignment, the performance gains through exploiting multi-user diversity in scheduling are not consistent and are highly topology dependent. By excluding fading statistics in routing and slot assignment, in the derived routing scheme, several nodes may use only one link to send their own and forward traffic for other nodes. These nodes of course cannot exploit multi-user diversity.

The gains, nevertheless, will be more consistent and less topology dependent if we use the proposed Framework-C that considers the shot-term fading statistics in the long-term routing and capacity planning. Fig. 6 shows that

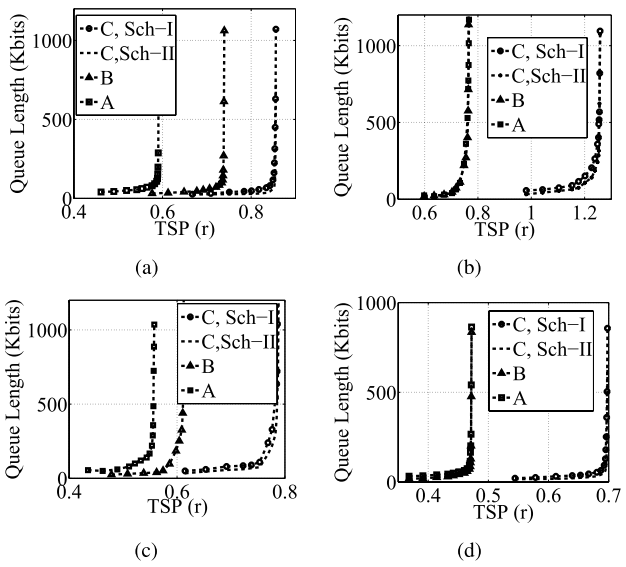

Fig. 6. Delay/throughput performances of the three frameworks, where delay is represented by the queue length of the bottleneck link: (a) 15-node network; (b) 20-node network; (c) 25-node network; (d) 30-node network.

Framework-C has an achievable throughput gain of 44.7%, 64.0%, 41.4% and 47.9% over Framework-A for the 15-node, 20-node, 25-node and 30-node network respectively, and a throughput gain of 15.8%, 64.0%, 28.5% and 47.9% over Framework-B for the 4 tested networks respectively.

VI. Conclusion

In this study, we propose a node-based opportunistic routing and scheduling scheme. In the proposed scheme, slot assignment, routing and scheduling are jointly optimized, which can explore multi-user diversity thoroughly and provide significant throughput gain compared with the static node-based and the hybrid node-based scheme [1]. To derive an efficient solution for the proposed scheme, a heuristic algorithm is also proposed. According to the results, even with the heuristic algorithm, the proposed node-based opportunistic routing and scheduling scheme can provide 15.8% to 64.0% higher throughput than that of the hybrid node-based scheme for the tested topologies. Moreover, the performance gain of the proposed scheme over the static node-based scheme is 38.4% to 64.0% for the teste topologies.

Appendix

A. CSI Feedback in a Frame

To construct a control sub-frame for CSI feedback, in this part, we first show the formulation of a link-based scheme.

$$\max \quad r \tag{15a}$$

$$\text{s.t.} \quad \sum_{\{f \in F\}} h_f x_{fe} \leq \sum_{\{L | e \in L\}} \zeta^L c_e^L \tag{15b}$$

$$(7), (10) \tag{15c}$$

Here ζ^L is the amount of time assigned to link pattern L in a frame, and c_e^L is the transmission rate of link e when

link pattern L is activated. The formulation of the node-based scheme based on the long-term channel statistics can be calculated according to (21) in [1]. As to CSI feedback, the traffic demand for each link is known (no routing scheme is needed). Hence we can modify (15) and use the following LP to compute the activation time for all the link patterns.

$$\min \quad \sum_{L \in LP} \rho^L \tag{16a}$$

$$\text{s.t.} \quad td_e \le m \sum_{\{L|e \in E^L\}} \rho^L c_e^L \tag{16b}$$

Here ρ^L is the number of slots of link pattern L required for CSI feedback. To construct a control sub-frame, the frame generation method discussed in Sec. III-D is not efficient as the number of slots of a link pattern is usually very small, and quantize all ρ^L to an integer number at one time will result in unnecessarily high bandwidth waste. We can then use the following method to produce a control sub-frame.

Let $\{\tilde{\rho}^L\}$ be the lower bound of $\{\rho^L\}$. Initially we set $\tilde{\rho}^L = 0$ for every L in the link patterns. Let function $frac(x)$ takes the fractional part of a real number x. The method then iterates between two steps:

1) Solve (16) by setting $\{\tilde{\rho}^L\}$ as the lower bound of (16);
2) Among all ρ^L, find the one with the largest $frac(\rho^L)$ (denote such a link pattern as L^*), set $\tilde{\rho}^{L^*} = \tilde{\rho}^{L^*} + 1$. If $\{\tilde{\rho}^L\}$ is a feasible solution of (16) output $\{\tilde{\rho}^L\}$; otherwise go to 1.

B. Expression of $E(y)$ and $Var(y)$ in (5)

The detailed derivation of $E(y)$ and $Var(y)$ is discussed in [20]. Here we only show the expression of them. $E(y) = det(I_{2N_{sc}} - 2\sigma^2 K P^{(m)})^{-\frac{1}{2}}$, where $\sigma^2 = \gamma^{N,e,k}$, $K = \frac{1}{2}\begin{bmatrix} Re(C) & -Im(C) \\ Im(C) & Re(C) \end{bmatrix}$. C is a matrix whose $(\cdot)_{ij}$ element is $C_{ij} = E(h_i(rx,tx)h_j(rx,tx)^*)$ and $h_i(rx,tx)$ is the channel gain of ith subcarrier between receiver rx and transmitter tx.

$$Var(y) = \frac{1}{N_{sc}^2} \sum_{i=1}^{N_{sc}} \sum_{j=1}^{N_{sc}} \det(I_{2N_{sc}} - 2\sigma^2 K Q_{ij}^{(m)})^{-\frac{1}{2}} - E^2(y)$$

Here $P^{(m)} = \begin{bmatrix} R^{(m)} & 0_{N_{sc}} \\ 0_{N_{sc}} & R^{(m)} \end{bmatrix}$, $Q_{ij}^{(m)} = \begin{bmatrix} S_{ij}^{(m)} & 0_{N_{sc}} \\ 0_{N_{sc}} & S_i j^{(m)} \end{bmatrix}$, $R^{(m)} = \text{diag}([-\beta_m^{-1}, 0, \cdots, 0])$, $S_{ij}^{(m)} = \text{diag}(A_{ij})$, and A_{ij} is a $1 \times N_{sc}$ vector whose elements are all 0 except that the ith and jth element is â Ł" β_m^{-1} if $i \neq j$ and â Ł" $2\beta_m^{-1}$ if $i = j$.

C. Heuristic Algorithm of the Proposed Framework

1) Reduce the Number of States in a Node Pattern: Note that the number of states of node p in node pattern N increases exponentially with $|E_p^N|$. However, it is possible that the value of some state $g(s_p^N)$ is negligible. To reduce the number of states in a node pattern, we only consider the set of states $(\tilde{S}_p^N)$ that satisfy the following conditions:

$$\tilde{S}_p^N = \left\{ g(s_p^N) \mid g(s_p^N) \ge \delta_1, \sum_{s \in \tilde{S}_p^N} g(s_p^N) \ge 1 - \delta_2 \right\} \tag{17}$$

Here δ_1 and δ_2 are two small positive numbers. We set $\delta_2 = 0.01$ and search the largest δ_1 and $\tilde{S}_p^N$ that satisfy (17).

2) Determine the Set of Links Associated With Each Transmitting Node (E_p^N): Moreover, due to the marginal diminishing effect, the throughput gain due to the increase of $|E_p^N|$ is trivial. Nevertheless, the number of states in $\tilde{S}_p^N$ grows exponentially with the increase of $|E_p^N|$. Hence we set a limit on the maximum number of edges that can be attached to a transmitting node (denoted as e_{max}). Among all the links in E_p^N, we only choose e_{max} edges at most such that the resulting reduced price is the largest.

3) Determine the Modulation Scheme Groups of All the Links Associated With Each Transmitting Node: Denote the set of edges selected for node p in N as $\tilde{E}_p^N$. Since e_{max} and ξ are relatively small numbers, we then exhaustively search all the possible groupings and choose the one with the highest reduced price.

4) Determine the Node Pattern to be Added Into the Master Problem: With the previous techniques, we can reduce the problem size to a large extent. However, the number of node patterns is still too large; i.e., if there are n nodes in the network, there will be 2^{n-1} node patterns in the system. It is impossible to search all the node patterns in the sub-problem. Hence we propose to use a heuristic algorithm to search a new node pattern in each iteration.

The algorithm maintains two node sets denoted as Z and T, which are initialized to the entire node set V and an empty set Φ respectively. Let N_p be the newly generated node pattern and T be the set of transmitting nodes in N_p. N_p, initialized to Φ, is constructed by adding one node from Z to T iteratively.

1) Select any node $t \in Z$. Choose the link set associated with node t as well as the corresponding modulation groups for each link in the set so that the resulting reduced price is the largest.
2) Replace N_p with N_p', if $rp^{N'} < rp^N$.
3) Remove t from Z. If Z is empty, terminate the algorithm; otherwise, go to step 1.

D. The Detailed Result of Each Implementation Step

For brevity, the discussion on the throughput scaling parameter was left out in Sec. V-B.4. It is given below. The detailed throughput scaling parameters derived from every implementation step listed in Sec. V-B.4 are shown in Table III. Since the differences between the analytical results from Framework-A and Framework-B are small, we only present the results of Framework-B. In the table, the following notations are used:

1) r_A:the throughput scaling parameter derived from (21) in [1] for Framework-A;
2) r_C^{opt}/r_C^{heu}: the throughput scaling parameter derived from the optimal/heuristic algorithms (refer to Sec. V-B.1 for more details) for Framework-C;

TABLE III
THE THROUGHPUT SCALING PARAMETER OF EACH STEP

		15	20	25	30
Framework-A	r_A	0.634	0.895	0.655	0.567
	r_A^{adj}	0.630	0.885	0.643	0.573
	r_A^{quan}	0.616	0.853	0.619	0.532
	r_A^{CSI}	0.601	0.828	0.582	0.485
	r_A^{real}	0.592	0.767	0.558	0.468
Framework-B	r_B^{real}	0.739	0.767	0.614	0.468
Framework-C	r_C^{opt}	0.943	1.462	NA	NA
	r_C^{heu}	0.927	1.408	0.935	0.841
	r_C^{adj}	0.938	1.402	0.959	0.822
	r_C^{quan}	0.909	1.366	0.881	0.774
	r_C^{CSI}	0.889	1.309	0.840	0.602
	r_C^{real}	0.856	1.258	0.789	0.692

3) r_A^{adj}/r_C^{adj}: the throughput scaling parameter with the exact EESM distribution of Framework-A/C;
4) r_A^{quan}/r_C^{quan}: the throughput scaling parameter after quantizing the activation time of each node pattern to an integer number of slots (step 4 of Sec. V-B.4) of Framework-A/C;
5) r_A^{CSI}/r_C^{CSI}: the throughput scaling parameter with CSI feedback overhead of Framework-A/C;
6) $r_A^{real}/r_B^{real}/r_C^{real}$:the throughput scaling parameter with real scheduling and CSI feedback of Framework-A/B/C.

REFERENCES

[1] W. Chen and C.-T. Lea, "A node-based time slot assignment algorithm for STDMA wireless mesh networks," *IEEE Trans. Veh. Technol.*, vol. 62, no. 1, pp. 272–283, Jan. 2013.

[2] P. H. Pathak and R. Dutta, "A survey of network design problems and joint design approaches in wireless mesh networks," *IEEE Commun. Surveys Tut.*, vol. 13, no. 3, pp. 396–428, 2010.

[3] D. Allen, *Hidden Terminal Problems in Wireless LAN's*, IEEE Standard 802.11, Working Group Papers 802.11/93-xx, 1993.

[4] R. Nelson and L. Kleinrock, "Spatial TDMA: A collision-free multihop channel access protocol," *IEEE Trans. Commun.*, vol. COM-33, no. 9, pp. 934–944, Sep. 1985.

[5] M. J. Lee, J. Zheng, Y.-B. Ko, and D. M. Shrestha, "Emerging standards for wireless mesh technology," *IEEE Wireless Commun.*, vol. 13, no. 2, pp. 56–63, Apr. 2006.

[6] J. Gronkvist, J. Nilsson, and D. Yuan, "Throughput of optimal spatial reuse TDMA for wireless ad-hoc networks," in *Proc. IEEE 59th Veh. Technol. Conf., VTC Spring*, May 2004, pp. 2156–2160.

[7] P. Bjorklund, P. Varbrand, and D. Yuan, "Resource optimization of spatial TDMA in ad hoc radio networks: A column generation approach," in *Proc. 22nd Annu. Joint Conf. IEEE Comput. Commun. Soc. (INFOCOM)*, Mar. 2003, pp. 818–824.

[8] J. Gronkvist, "Traffic controlled spatial reuse TDMA in multi-hop radio networks," in *Proc. 9th IEEE Int. Symp. Pers., Indoor Mobile Radio Commun.*, Sep. 1998, pp. 1203–1207.

[9] T. Moscibroda, R. Wattenhofer, and A. Zollinger, "Topology control meets SINR: The scheduling complexity of arbitrary topologies," in *Proc. 7th ACM Int. Symp. Mobile ad hoc Netw. comput.*, 2006, pp. 310–321.

[10] S. Kompella, J. E. Wieselthier, A. Ephremides, H. D. Sherali, and G. D. Nguyen, "On optimal SINR-based scheduling in multihop wireless networks," *IEEE/ACM Trans. Netw.*, vol. 18, no. 6, pp. 1713–1724, Dec. 2010.

[11] P. Santi, R. Maheshwari, G. Resta, S. Das, and D. M. Blough, "Wireless link scheduling under a graded SINR interference model," in *Proc. 2nd ACM Int. Workshop Found. Wireless ad hoc Sensor Netw. Comput.*, 2009, pp. 3–12.

[12] S. Fan, L. Zhang, Y. Ren, and B. Krishnamachari, "Approximation algorithms for link scheduling with physical interference model in wireless multi-hop networks," in *Proc. IEEE 48th Annu. Allerton Conf. Commun., Control, Comput. (Allerton)*, Sep. 2010, pp. 522–529.

[13] P. Djukic and S. Valaee, "Delay aware link scheduling for multi-hop TDMA wireless networks," *IEEE/ACM Trans. Netw.*, vol. 17, no. 3, pp. 870–883, Jun. 2009.

[14] M. Johansson and L. Xiao, "Cross-layer optimization of wireless networks using nonlinear column generation," *IEEE Trans. Wireless Commun.*, vol. 5, no. 2, pp. 435–445, Feb. 2006.

[15] W. Chen and C.-T. Lea, "Energy conservation routing in multi-hop wireless networks," *IEEE Trans. Veh. Technol.*, vol. 64, no. 8, pp. 3633–3644, Aug. 2015.

[16] C. Eklund *et al.*, "IEEE standard 802.16: A technical overview of the wirelessman air interface for broadband wireless access," *IEEE Commun. Mag.*, vol. 40, no. 6, pp. 98–107, Jun. 2002.

[17] B. Sadeghi, V. Kanodia, A. Sabharwal, and E. Knightly, "Opportunistic media access for multirate ad hoc networks," in *Proc. 8th Annu. Int. Conf. Mobile Compu. Netw.*, Sep. 2002, pp. 24–35.

[18] M. Vutukuru, H. Balakrishnan, and K. Jamieson, "Cross-layer wireless bit rate adaptation," in *Proc. ACM SIGCOMM Comput. Commun. Rev.*, 2009, pp. 3–14.

[19] D. Tse and P. Viswanath, *Fundamentals of Wireless Communication*. Cambridge, U.K.: Cambridge Univ. Press, 2005.

[20] J. Francis and N. B. Mehta, "Eesm-based link adaptation in point-to-point and multi-cell ofdm systems: Modeling and analysis," *IEEE Trans. Wireless Commun.*, vol. 13, no. 1, pp. 407–417, Jan. 2014.

[21] N. Wiener, *The Fourier Integral and Certain of Its Applications*. Cambridge, U.K.: Cambridge Univ. Press, 1988.

[22] B. Ji, C. Joo, and N. B. Shroff, "Throughput-optimal scheduling in multihop wireless networks without per-flow information," *IEEE/ACM Trans. Netw.*, vol. 21, no. 2, pp. 634–647, Apr. 2013.

[23] E. Westman, "Calibration and evaluation of the exponential effective SINR mapping (EESM) in 802.16," in *Proc. Masters Degree Project*, 2006, pp. 7–9.

[24] J. Salo *et al.*, "Matlab implementation of the 3GPP spatial channel model," in *Proc. GPP TR*, 2005, p. 966.

[25] B. P. Crow, I. Widjaja, J. G. Kim, and P. T. Sakai, "IEEE 802.11 wireless local area networks," *IEEE Commun. Mag.*, vol. 35, no. 9, pp. 116–126, Sep. 1997.

[26] I. F. Akyildiz, X. Wang, and W. Wang, "Wireless mesh networks: A survey," *Comput. Netw.*, vol. 47, no. 4, pp. 445–487, Mar. 2005.

Weiwei Chen received the B.S. degree in electronic engineering from the Beijing University of Posts and Telecommunications University, Beijing, China, in 2007, and the Ph.D. degree from The Hong Kong University of Science and Technology, Hong Kong, in 2013. She is currently with the College of Computer Science and Electronic Engineering, Hunan University, China. Her research interests include mobile cloud computing, cross-layer optimizations in wireless networks, 5G cellular networks, and future internet architecture.

Chin-Tau Lea received the B.S and M.S. degrees from National Taiwan University in 1976 and 1978, respectively, and the Ph.D. degree from the University of Washington, Seattle, WA, USA, in 1982, all in electrical engineering. He was with the AT&T Bell Labs from 1982 to 1985. He was with the Georgia Institute of Technology from 1985 to 1995. He has been a Professor with The Hong Kong University of Science and Technology since 1996. His research interests are in the general area of switching and networking. His major research contributions include the invention of multi-Log2N networks and the associated crosstalkfree photonic switching theory, and the original work on the design of uncertainty tolerant networks.

Shiming He received the Ph.D. degree from Hunan University, Changsha, China, in 2013. She is currently with the Department of Computer Science, Changsha University of Science and Technology. Her research interests include WMN, SWIPT, and opportunistic routing.

Zhe XuanYuan received the B.S. degree in electronic engineering from Peking University, Beijing, China, and the Ph.D. degree from the Internet Switching Technology Laboratory, Department of Electronic and Computer Engineering, The Hong Kong University of Science and Technology. He was with Sun Yat-sen University from 2014 to 2016. He was with Huawei from 2012 to 2014. He has been an Assistant Professor with United International College since 2016. His research interests include routing protocol design and analysis, network coding theory and application, algorithms for related optimization problems, future Internet architectures, and vehicular networks.